Geomechanics and Engineering, *Vol. 38, No. 6 (2024) 583-591*
https://doi.org/10.12989/gae.2024.38.6.583

Structural stability evaluation of TBM tunnels using numerical analysis approach

Dohyun Kim*

Department of Civil and Environmental Engineering, Hanbat National University, Daejeon 34158, Korea

(*Received December 7, 2023, Revised February 12, 2024, Accepted February 23, 2024*)

Abstract. To properly simulate the excavation process and evaluate the structural stability of the tunnel, rigorous large deformation analysis method is necessary. This study applies two most widely used numerical approaches capable of modelling and considering the large deformations behavior during excavation process to analyze and evaluate the structural stability of circular tunnel based on tunnel boring machine (TBM) excavation. By comparing and combining the results from two numerical approaches, the deformation of the excavated ground will be analyzed. The stability of the circular tunnel from TBM tunneling was assessed based on the maximum deformation occurred during the excavation process. From the numerical computation it was concluded that although the range of the damage on the ground done during excavation was found to be larger under hard rock condition, maximum deformation within the circular tunnel structure was larger under weak ground conditions and deeper tunnel depths.

Keywords: circular tunnel; large deformation analysis; numerical analysis; TBM tunnels; tunnel deformation

1. Introduction

As the urbanization accelerates, the needs for underground space development rose in various field of society – transportation, commercial and various lifelines (water, electric, gas, etc.). However, the application of conventional tunneling method in concentrated urban areas is not a viable option due to the noise and vibration during excavation. The noise can cause numerous legal issues towards the construction project, as well as extend the construction period of the project. Moreover, numerous observations on the negative effects on the surrounding structures and resident quality were reported through research projects and literatures. This is a major concern since in modern urban areas a minor negative incident can lead to massive financial loss as well as human lives.

Substitution of the conventional tunneling method, like drill-and-blast method, to mechanized tunnel boring machine (TBM) tunneling method is one of the movements to deal with the limitations mentioned in the previous paragraph. However, compared to the studies conducted on the structural stability of tunnels excavated under conventional tunneling method, studies on the structural stability or behavior of tunnels excavated based on mechanized tunneling method has not been carried out on an adequate number of cases.

Numerous institutes, such as Underground Research Laboratory (URL) (Canada), Swedish Nuclear Fuel and Waste Management Corporation (SKB) (Sweden) and Korean Atomic Energy Research Institute (KAERI) (Korea), studied and investigated excavation damage zone (EDZ) around the excavation surface, and on the changes in physical and material properties (Bauer *et al.* 1996, Emsley *et al.* 1997, Martin *et al.* 1997, Read *et al.* 1998, Kwon *et al.* 2009) through theoretical and experimental approaches.

The formation of the EDZ is found to be critical to the tunnel's structural stability during excavation and in-service period due to the changes in physical and mechanical property compared to the original rock mass (Stepansson *et al.* 2008, Arson and Gatmiri 2012, Siren 2015). Moreover, the behavioral characteristics of the EDZ around the excavation surface were found to be closely associated with the tunnel geometry, as well as the dynamic response of the surrounding ground. The blast vibration caused during the conventional drill and blast method, as well as the vibration due to the advancement of the TBM are found to cause severe damage to the ground which will reduce the strength and stability of the ground and the tunnel (Siren 2015).

Although numerous studies were carried out on the EDZ around the tunnel excavation surface, most of the studies and field measurements were focusing on conventional drill and blast method. On the contrast, very few studies were on mechanized tunnels, and attempts to predict the distribution and the range of the EDZ based on numerical analysis were not actively carried out (Read *et al.* 1998, Carbonell *et al.* 2010, Xu and Arson 2014, Lee *et al.* 2016, Chen *et al.* 2023, Lee *et al*. 2023).

In analyzing the behavior of TBM tunnels during excavation, the latest studies mainly consider the behavior of rock mass during excavation and interaction of the rock mass with the TBM and tunnel lining (Zhao *et al.* 2012). However, the numerical analysis conducted up to date were based on static, discrete sequential analysis, which lacks the capacity in simulating and analyzing the actual dynamic and continuous behavior of the TBM excavation process.

*Corresponding author, Assistant Professor
E-mail: geokim@hanbat.ac.kr

http://www.techno-press.org/?journal=gae&subpage=7
ISSN: 2005-307X (Print), 2092-6219 (Online)

Conventional numerical analysis method (small deformation analysis) has limited capacity in solving the contact surface problems and the excessive deformation of the mesh as the tunnel excavates. To overcome these limitations, and accurately analyze the dynamic behavior of the ground-structure interaction under continuous excavation process, the use of large deformation analysis is necessary (Kim 2021, Kim *et al.* 2023). This will lead to rigorous analysis on the structural stability of tunnels based on mechanized method.

In this study, the structural stability of circular TBM tunnels will be investigated and quantified associated with excavation damage zone (EDZ) in the surrounding ground. The stability of the circular tunnel will be numerically analyzed by using two most widely applied large deformation analysis method – coupled Eulerian-Lagrangian (CEL) and auto-remeshing method. After numerically simulating the TBM excavation process the damage on the surrounding ground will be computed along with the maximum deformation in tunnel's excavation surface under the condition without the tunnel lining, which will be the indicator on the structural stability of the tunnel. This will be investigated for various ground conditions (RMR rating) and tunnel depths.

2. Excavation damage zone

Redistribution of initial stress around the tunnel occurs and fractures and cracks form in the rock mass during the excavation process. The definition associated with damaged zones caused by excavation are summarized as shown in Fig. 1 (Perras and Diederichs 2016). Harrison and Hudson (2000) use the terminology of construction damage zone (CDZ), where an inevitable excavation consequences and additional effects occur due to excavation. However, the CDZ can be neglected in most mechanized tunnelling process, due to its insignificant range. Zone where it undergoes inevitable damages caused by the result of geometry, structure, and/or induced stress changes (i.e., independent of excavation method) can be defined as the highly damaged zone (HDZ). The HDZ can be typically observed as a zone including interconnection of micro-fractures. Outside the HDZ is normally called the excavation damaged zone (EDZ). The definition of EDZ usually refers to as an area or zone around the excavation surface, where the changes in stress due to excavation exceeds the elastic limit and newly formed fractures or cracks occur. EDZ appears as the tunnel excavates by cracking the rock mass, and this causes reduction of strength and stability of surrounding grounds (Martino *et al.* 2007, Sun *et al.* 2023). Siren *et al.* (2015) introduced a concept of excavation influence zone (EIZ), or excavation disturbed zone (EdZ), where it only involves elastic changes degree of stress redistribution.

Hoek and Bieniawski (1965) presented the results of the laboratory test on the initiation of a fracture of brittle materials, such as rocks. For materials under uniaxial compression loading condition, the initiation of fracture occurred at about 800% of maximum tensile strength of the material. Additional tests were conducted on various rock types, and the results show that the initiation of fracture occurred at 1500 - 2000% of maximum tensile strength. Martin (1993) and Martin *et al*. (2001) defined the stages in the progressive failure of rock and suggested an equation which designates the EDZ around the tunnel based on the field stress ratio. Diederichs *et al*. (2004) reported an experiment-based field stress ratio (FSR), to determine the crack initiation stress for various rock types. Saiang (2004) suggested a model to estimate the EDZ based on field measurements and conducted a series of study on the main influence factors on EDZ. Swedish nuclear fuel and waste management conducted a project ZEDEX – Zone of Excavation Disturbance EXperiments – to specify the characteristics of EDZ and their behavior and effect on rock conditions due to mechanized excavation as well as conventional tunnelling. Siren (2015) compared the difference in the distribution shape and magnitude of EDZ between NATM and TBM tunnels, along with the changes in mechanical properties through field measurements. Some studies attempted to simulate the formation of the EDZ around the mechanized tunnel surface using particle finite element method (PFEM) (Carbonell e*t al*. 2010). Nevertheless, it can be pointed out that most studies have focused on experiments and field measurements after the excavation of the tunnel in defining the EDZ. By contrast, the estimation and prediction of the EDZ using dynamic three-dimensional finite element (FE) method and discussing the relationship between the formation of the EDZ and the stability of the tunnel through numerical evaluation have not been thoroughly presented.

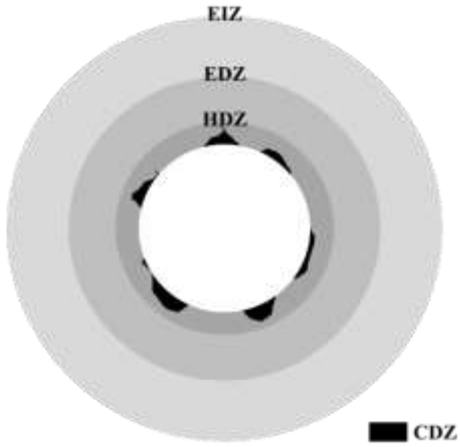

Fig. 1 Various excavation damage zones

The development of the EDZ around the tunnel excavation surface is critical to the stability during tunnel construction process and the tunnel structure after the completion. Diederichs *et al.* (2004) conducted experiments to define the crack initiation of various rock types, Martin *et al.* (1993, 2001) suggested a simple equation (Eq. (1)) that under axial loading condition the crack initiation stress is approximately 30 - 40% of the rocks' uniaxial compression strength based on the field stress ratio results (Fig. 2).

$$\sigma_1' - \sigma_3' = \sigma_{ci} = 30 - 40\%\ of\ UCS \quad (1)$$

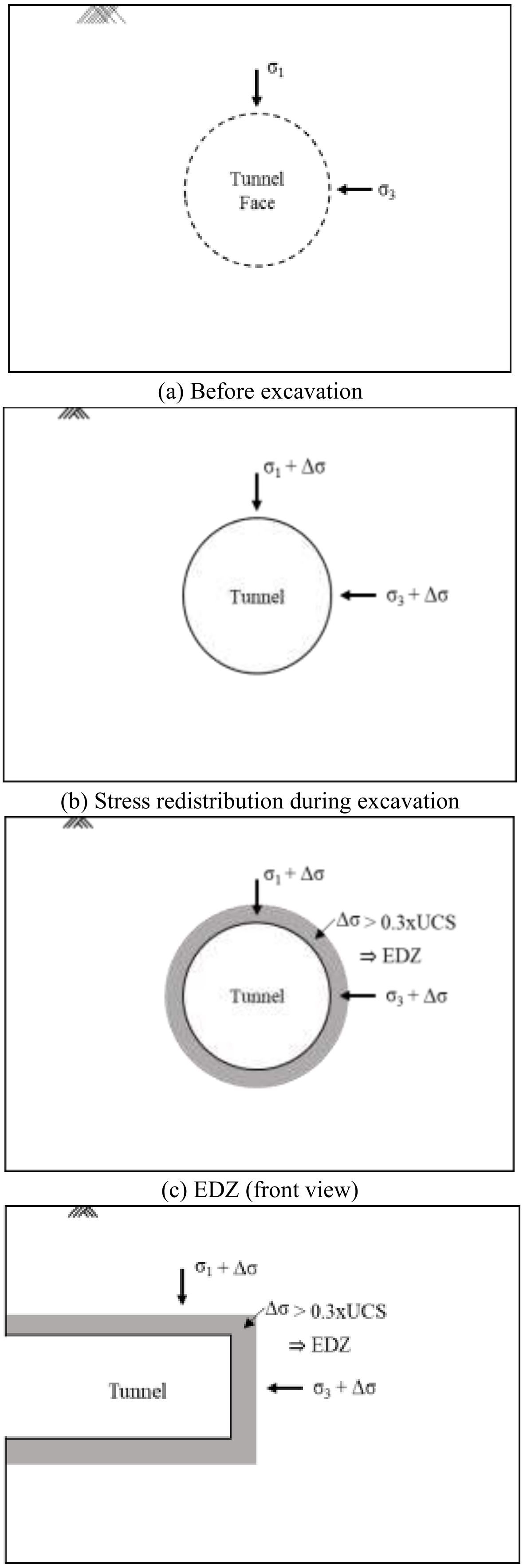

(a) Before excavation

(b) Stress redistribution during excavation

(c) EDZ (front view)

(d) EDZ (side view)

Fig. 2 Formation of the EDZ during tunnel excavation

where, σ_{ci} is the crack initiation stress. Based on the Eq. (1), this study has defined the EDZ as an area where the deviatoric stress ($\sigma_1' - \sigma_3'$) caused by the excavation and the dynamic load due to vibration exceeds 30% of the ground's uniaxial compressive strength. This is the lower boundary of the definition of the crack initiation stress based on the field stress ratio, and yield larger EDZ around the excavation surface, thus allowing a safer tunnel design and maintenance. As the tunnel excavation is in progress, the initial stress (σ_1 or σ_3) around the excavation surface changes ($\sigma_1 + \Delta\sigma$). As the excavation continues, the deviatoric stress ($\Delta\sigma$) increases. In this study the same assumption is made that, when the deviatoric stress exceeds 30% of the original rocks' uniaxial compression strength, new cracks are formed, thus EDZ appears around the tunnel excavation surface. By using large deformation analysis, the range and the distribution shape of the EDZ under various conditions are investigated along with the stability assessment based on the maximum deformation within the excavation surface.

3. Numerical modeling and analysis

3.1 Mesh and boundary conditions

In finite element analysis, the plasticity of soil is considered through constitutive model, and the most common constitutive model for rock is Mohr-Coulomb model and the Hoek-Brown model. In this study, the Mohr-Coulomb model was used to analyze the behavior of rocks for both analytical approaches. The element type for the CEL mesh is set to Eulerian element (EC3D8R).

The interface between the Eulerian and Lagrangian elements for CEL analysis are commonly modelled as a general contact. In this study, the interface between the elements (cutterhead or lining with the rock mass) are modelled as a general contact for CEL as well as the auto RITSS method. The friction coefficient between the elements are set to 0.7, based on previous studies (Gehring 1996, Zhao *et al*. 2012, Ramoni and Anagnostou 2011).

The size of the mesh boundary was modeled to prevent the boundary disturbance effect. The length along the x- and y- direction was 14 m (5D) and 14 m (5D) respectively, where D is the diameter of the tunnel, 3.5 m. The size of the mesh in z-direction differs by the tunnel depth, while maintaining at least 5D space above and below the excavation surface.

The size of the single mesh affects the accuracy and the computation time of the analysis. Using smaller mesh size may increase the accuracy of the analysis. However, it also significantly increases the computation time. Convergence study in order to select the ideal mesh size was carried out prior to the actual analysis. According to the convergence study results, mesh size of 10 cm was found to provide consistent results under reasonable compute time. Dense mesh was distributed in the 1D range around the excavation surface, and the mesh size gradually increased as the distance from the excavation surface increases, to secure the accuracy of the results while maintaining reasonable compute time.

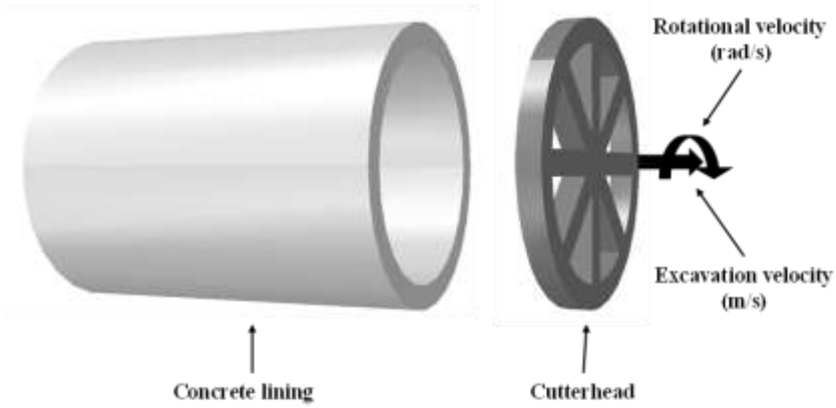

Fig. 3 Schematic of the modeling of TBM cutterhead and lining

Table 1 Material property of ground (rock) based on RMR ratings (Jeong *et al.* 2014)

Grade	RMR	UCS (MPa)	E (MPa)	v	γ (kN/m3)	φ (°)	c (kPa)
1st grade	80~100	75	20,000	0.2	27	45	4,000
2nd grade	61~80	50	10,000	0.22	26	40	2,000
3rd grade	41~60	30	6,000	0.24	25	35	1,000
4th grade	21~40	10	2,000	0.26	23	32	400
5th grade	< 20	4	800	0.28	22	30	100
Weathered rock	-	2	200	0.30	21	32	50

Table 2 Material property of cuterhead and lining (Kim 2021)

	Model (Element)	E (MPa)	v	γ (kN/m3)	φ (°)	c (kPa)
Lining	Linear elastic (C3D8R)	23,000	0.15	24.0	-	-
Cutterhead		200,000	0.30	82.5	-	-

The material properties of the rock based on RMR ratings are summarized in Table 1 (Jeong *et al.* 2014).

3.2 TBM and lining modeling

Model The modeling of the tunnel boring machine (TBM), which consists of the cutterhead and the lining, is based on a Lagrangian framework for both CEL and auto RITSS analysis. The properties of the TBM are stated in Table 2 (Kim, 2021). The TBM elements are modeled as an 8-node Lagragian brick element (C3D8R) linear elastic material – assumed as a rigid element. This will eliminate the effect of additional deformation or stress issues, and solely focus on the effect of ground excavation. The initial tunnel length is set to 5m, and the initial geostatic conditions are set accordingly. Fig. 3 shows the TBM cutterhead and lining modeled based on Lagrangian element.

3.3 TBM excavation

The main purpose of using the CEL in TBM advancement and excavation is to simulate the TBM movement closest to the actual TBM in practice. Using the coupled Lagrangian (TBM elements) and Eulerian (ground element) elements, the simulation of the TBM advancement can be achieved by actually 'cutting' and 'excavating' the ground, as the excavated particles (debris) are flown beyond the cutterhead.

The net velocity of the TBM advancement in the field is approximately $5x10^{-4}$m/s (ITA 2000). Adapting the quasi-static condition and through series of case studies, higher TBM advance velocity could be used in the analysis, and thus significantly reduce the computation time while not affecting the outcome of the results. Based on case studies, increasing the TBM advance velocity up to $1x10^{-3}$m/s did not affect the outcome compared to the actual advance velocity of $5x10^{-4}$m/s, while the computation time reduces dramatically. For this reason, the TBM velocity in this study was modelled to 10^{-3}m/s to estimate the EDZ around the excavation surface. In addition, the rotation rate of the cutterhead is set to 6rad/s (1RPM) based on field practice recommendations and previous studies (Lee *et al.* 2016; Kim and Jeong 2021, Kim 2021)..

Moreover, the effect of the TBM cutterhead excavating the ground was simulated based on the interface strength

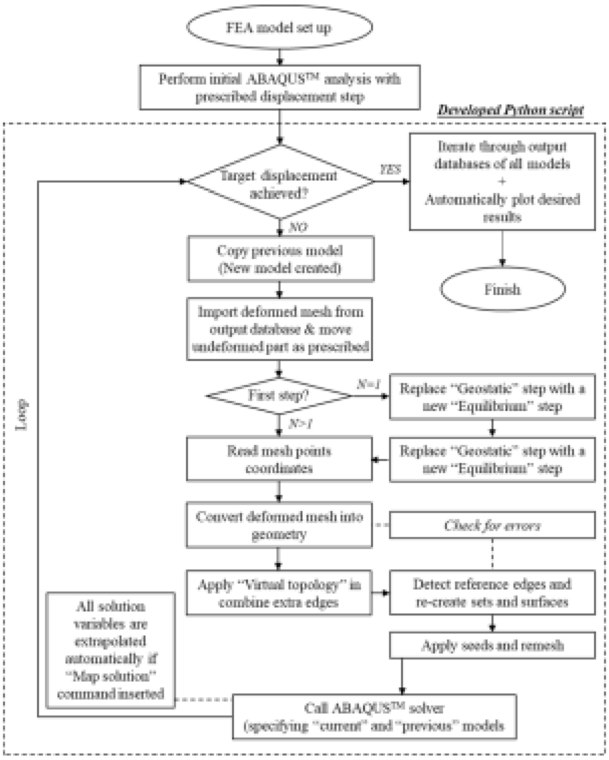

Fig. 4 Flow chart of analysis procedure Schematic of the modeling of TBM cutterhead and lining

reduction factor (R_{int}). Conventional value of the Rint when modelling a soil-structure interface is set between the values of 0.3 – 0.7 (0 is frictionless, and 1.0 a rigid contact). However, to simulate the high friction and the excavation process between the cutterhead – ground interface, the R_{int} value was set higher than an usual interface, to 0.9.

Auto-remeshing numerical approach can avoid severe mesh distortion and calculation failure under large deformation analysis by updating the finite element mesh and the stress state before the unwanted mesh distortion. Although the auto-remeshing approach is not capable of simulating the actual TBM advance and excavation in real-time as CEL method, it has been proved by numerous studies and research that it is capable of simulating and predicting the ground response during drilling and excavation (Hu and Randolph 1998, Tian *et al.* 2014, Wang *et al*. 2015).

The auto-remeshing method is applied by updating the mesh and the stress / state variables every 1 second, which complies with the TBM advance velocity selected by the case studies conducted prior to the actual analysis. The automated remeshing process is independently implemented using a set of object-oriented language, PYTHON script that can be used in ABAQUS scripting interface. The proposed procedure implemented in the scripts contain specification of multiple variables to a specific geometry, elements, boundary conditions, target displacement per single advance process ($1x10^{-3}$ m). The initial processes, which is model development and initial analysis, are done manually, using the CAE option. After the initial analysis (first 10^{-3} m excavation), the rest of the process is automated using the developed scripts. When the main script is called and applied for the first time, it checks whether the targeted

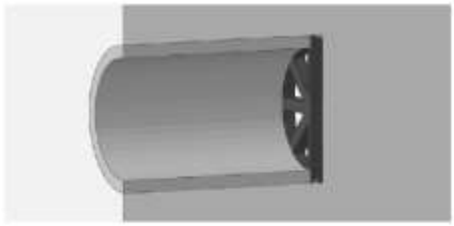

(a) Initial position

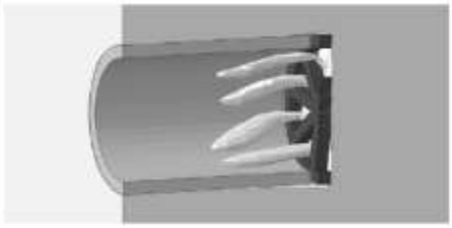

(b) 0.15 m excavation (150 steps)

(c) 0.30 m excavation (300 steps)

Fig. 5 Flowing of the Eulerian elements in CEL method

excavation length has been reached or not. If it is reached, a set of other scripts are applied to automatically iterate through all outputs of the previous step, considering the deformations and stresses occurred during the process. If the targeted excavation length is not reached, then a new

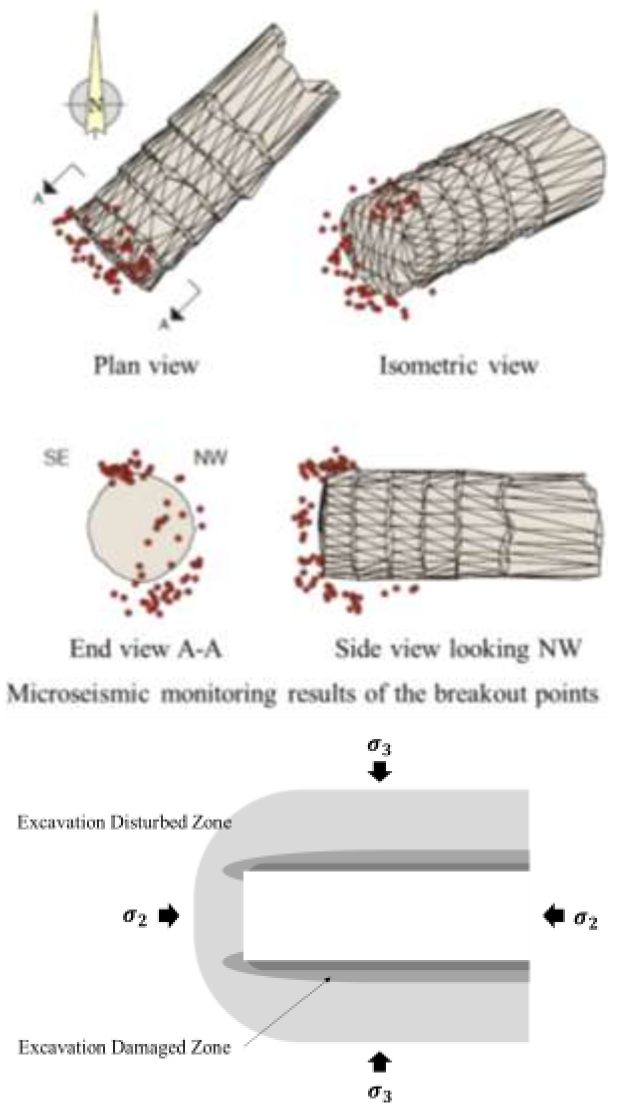

(a) Test results reported by Read (2004)

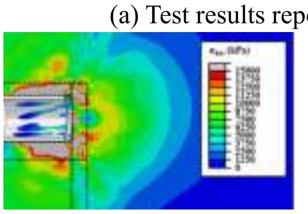
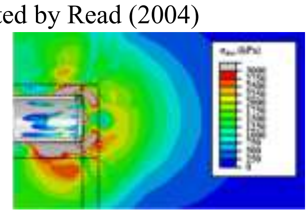

(b) CEL analysis

Fig. 6 Comparison of the measured numerical results

step and mesh is created by invoking the following ABAQUS scripting interface command:

Mdb.Model(name=*newmodel*,objectToCopy=mdb.models[*oldmodel*])

where, *oldmodel* is the variable containing the name of the previous model, and *newmodel* is the variable containing the new model name in which the step number is incrementally updated (i + 1) each step (Kim 2021). This process is continued till the targeted excavation length of 0.3 m, equivalent to 300th step, is reached (Fig. 4). It was shown in the results that after the 300th step the stress redistribution was stable and has converge to a certain degree.

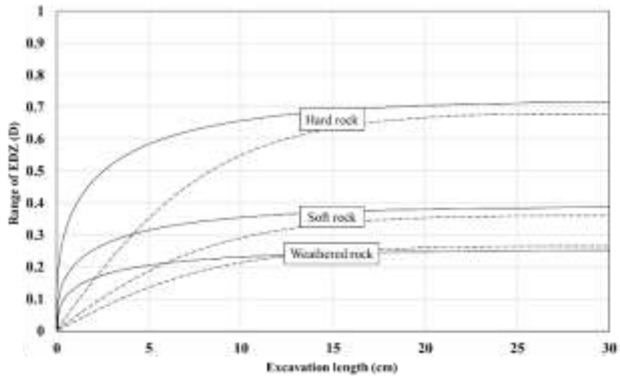

(a) Vertical direction

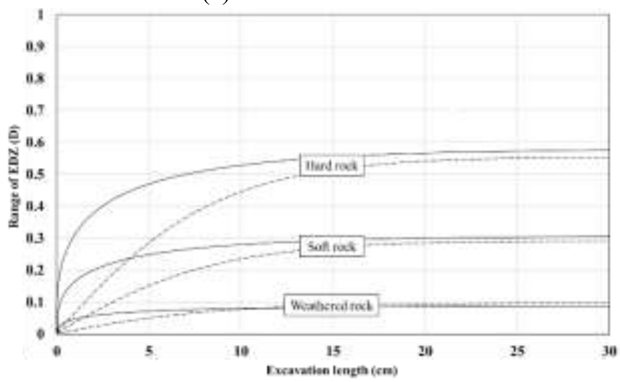

(b) Horizontal direction

Fig. 7 EDZ estimation results using LDA (5D depth)

The verification of the numerical model and the large deformation method applied in this study was carried out in the following chapter.

Fig. 6 displays the result comparison between the laboratory test and the computed results (Read, 2004). The pattern of the EDZ around the model-scale mechanized tunnel and the computed EDZ shape based on CEL simulation shows overall similarities – in both size and the distribution shape. It is clear that due to TBM excavation, the changes in stress is higher near the edge of the TBM cutterhead, forming a doughnut-like shape. The maximum range of the EDZ from the numerical calculation was in the range of 10% to 50% of the tunnel diameter (0.1D – 0.5D). These results were in good agreement with the previous studies and test results reported in literature (Martin 1989, Cundall *et al.* 1996, Martin *et al.* 1997, Diederichs *et al.* 2004, Martino and Chandler 2004).

Based on the verification process based on laboratory test results and previous studies, the numerical model applied in this study is capable of simulating the TBM excavation process and calculating the ground's response due to TBM excavation – the distribution shape and size of the EDZ around the excavation surface.

Additional indirect verification of the auto-remeshing method on the capacity of estimating the range of EDZ around the excavation surface.

Figs. 7-9 shows the results in estimating the EDZ around the excavation surface under various ground condition and tunnel depth. The results are categorized for

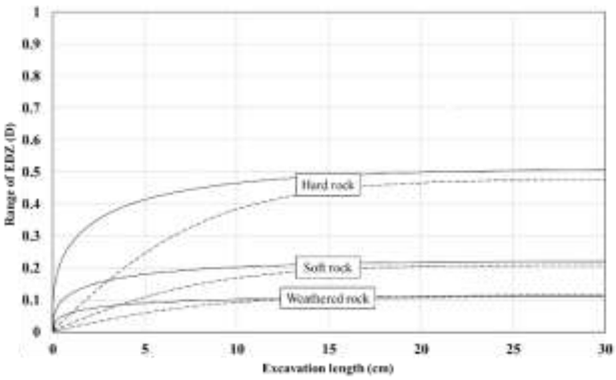

(a) Vertical direction

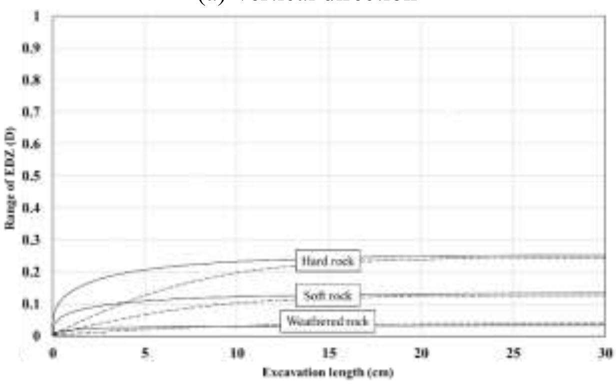

(b) Horizontal direction

Fig. 8 EDZ estimation results using LDA (10D depth)

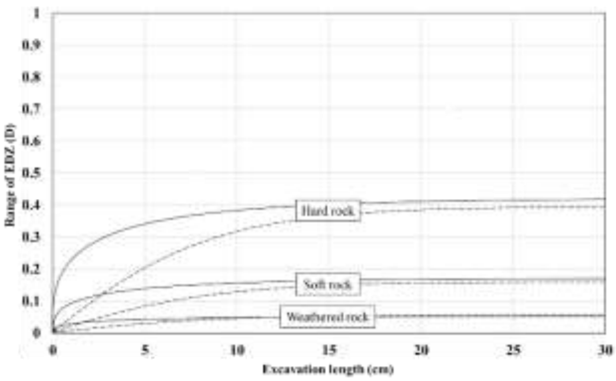

(a) Vertical direction

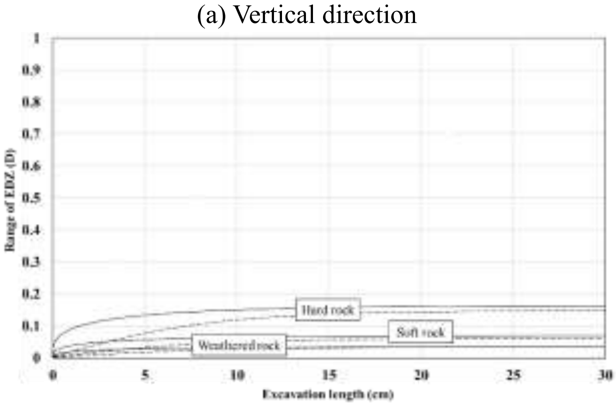

(b) Horizontal direction

Fig. 9 EDZ estimation results using LDA (20D depth)

vertical and horizontal direction. Based on the results, the maximum size of EDZ for vertical and horizontal direction show overall similar tendencies during TBM excavation. The difference in the earlier stages of estimation can be explained as a excessive formation of the damage zone due to actually tearing through the FEM mesh based on the CEL method. Whereas, in the auto-remeshing calculation, the formation of the EDZ is relatively gentle. However, the converging size of the maximum range of the EDZ around the TBM excavation surface is well observed.

For this reason, it can be concluded that the results based on the two large deformation analysis method used in this study reflects the damage and the reaction of the surrounding ground during TBM excavation.

4. Stability of TBM tunnels based on maximum deformation

Stability of the circular tunnel based on mechanized tunneling was evaluated and investigated, which may be critical and practical in actual tunnel engineering practice.

Based on observations and measurements by Sakurai (1983) and Chern *et al*. (1998), tunnels with strain level over 1% may be structurally instable associated with difficulties in providing adequate degree of support. Even though some tunnels which suffered strains exceeding 5% did not show stability problems, it was clear that construction problems increased significantly with increasing strain level over 1%. For this reason, the 1% limit in indicating the instability of tunnel was applied in the analyses due to excavation and stress redistribution (Fig. 10).

Table 3 shows the results of the maximum deformation of the tunnel through large deformation analysis. It was evidently shown that, even though larger size of the EDZ was estimated to form around the tunnel for harder rock conditions (Kim, 2021), the stability of the tunnel was not compromised for RMR 1^{st} rocks, where maximum deformation occurred during the excavation process was below 1%. In case of RMR 2^{nd} grade condition rocks, the maximum deformation along the tunnel excavation surface exceeded 1% only for tunnel with higher depth (20D). For RMR 3^{rd} grade condition, maximum deformation exceeding 1% only appeared all through the analysis cases. Based on these results, rocks of RMR 1^{st} through 3^{rd} grade was found to be overall stable, despite the wide range formation of the EDZ.

As for the rocks below the 4^{th} grade to weathered rock, maximum deformation caused by the TBM excavation was all over the 1% limit. Especially, in case of TBM excavation under weathered rock conditions, it showed to be extremely unstable, where the maximum deformation within some point among tunnel sectional area exceeded 20% during TBM excavation. In addition, the strain of the tunnel was found to be higher as the tunnel depth increases. This may be caused by the high in-situ earth pressure acting on the tunnel, where it is critical to install thorough linings and reinforcements (rock bolts, shotcrete, etc.) for deep tunnel excavation on relatively weaker ground condition.

Table 3 Material property of ground (rock) based on RMR ratings (Jeong *et al.* 2014)

Grade	Depth		
	5D (Max. deformation)	10D (Max. deformation)	20D (Max. deformation)
1st grade	Negligible (< 1%)	Negligible (< 1%)	Negligible (< 1%)
2nd grade	Negligible (< 1%)	Negligible (< 1%)	**1.6% / 1.6% / 1.4%**
3rd grade	< 1% / **1.1% / 1.1**	**1.0% / 1.3% / 1.3**	**2.0% / 2.2% / 2.2%**
4th grade	**3.6% / 3.6% / 3.5%**	**4.3% / 4.4% / 4.9%**	**5.0% / 5.0% / 5.2%**
5th grade	**5.2% / 5.5% / 6.0%**	**5.0% / 6.0% / 6.7%**	**8.3% / 9.1% / 9.0%**
Weathered rock	**11.8% / 12.6% / 12.7%**	**14.9% / 15.3% / 15.5%**	**22.9% / 23.5% / 23.7%**

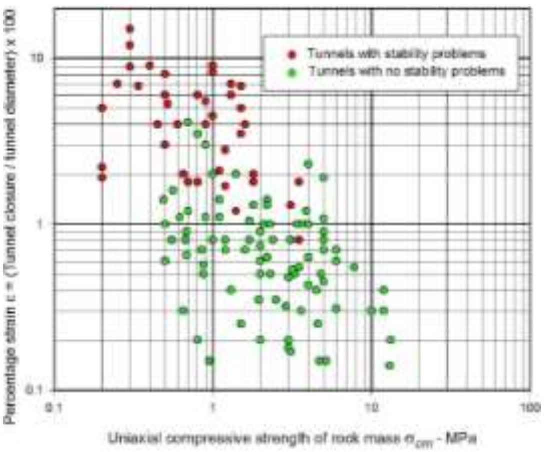

Fig. 10 Tunnel stability based on strain (Chern *et al.* 1998)

5. Conclusions

In this study, the structural stability of circular mechanized tunnels was investigated by using three-dimensional large deformation analysis method. The evaluation of the tunnel stability was conducted based on the maximum deformation among any location (point) within the tunnel excavation surface. By analyzing the strain level during TBM excavation, it was concluded that the formation of the EDZ does not always pose a threat to the tunnel's structural stability. Even though the size of the EDZ was shown to form largest in harder rock masses (RMR 1st – 3rd grade rocks) due to stress redistribution or faster and longer propagation of the TBM excavation vibration, the deformation occurred during the excavation was limited to 1%. As for the weaker rock masses, the EDZ was shown in smaller sizes, but there were certain points among the excavation surface where the maximum deformation exceeded the 1% limit – in weathered rock, up to 23% – which can be a clear indicator of decrease in structural stability.

Although the formation for the EDZ due to TBM excavation may be kept in limited sizes compared to the conventional drill-and-blast method, it can still cause significant degree of the EDZ around the excavation surface, as well as decrease in tunnel stability. For this reason, special attention and reinforcement during TBM operation is necessary, especially for TBM tunnels within deep depth below the surface on weak rock masses (i.e., below RMR 4th grade, including weathered rock).

In addition, this study focuses on – and is limited to – the structural stability of the tunnel associated with EDZ and maximum deformation during the TBM excavation process. Other issues related with the structural stability of the tunnel, such as rockbursts, were not considered in this study or numerical analysis.

The results estimated in this study's approach can be applied in providing safety assessment and geotechnical consideration in planning underground tunnels, highways and lifelines in urban areas.

References

Arson, C. and Gatmiri, B. (2012), "Thermo-hydro-mechanical modeling of damage in unsaturated porous media: Theoretical framework and numerical study of the EDZ", *Int. J. Numer. Anal. Method. Geomech.*, **36**(3), 272-306. https://doi.org/10.1002/nag.1005.

Bauer, C., Homand-Etienne, F., Ben Slimane, K., Hinzen, K.G. and Reamer, S.K. (1996), "Damage zone characterization in the near field in the Swedish ZEDEX tunnel using in situ and laboratory measurements", *Eurock '96, Balkema*, Rotterdam.

Carbonell, J., Onate, E. and Suarez, B. (2010), "Modeling of ground excavation with the particle finite-element method", *ASCE J. Eng. Mech.*, **136**(4), 455-463. https://doi.org/10.1061/(ASCE)EM.1943-7889.000008.

Chen, L., Lu, L., Tang, Z., Yi, S., Wang, Q. and Chen, A. (2023), "Effects of parallel undercrossing shield tunnels on river embankment: Field monitoring and numerical analysis", *Geomech. Eng.*, **35**(1), 29-39. https://doi.org/10.12989/gae.2023.35.1.029.

Chern, J.C., Yu, C.W. and Shiao, F.Y. (1998), "Tunnelling in squeezing ground and support estimation", *Proceedings of the Regular Symposium of Sedimentary Rock Engineering*, Taipei.

Cundall, P.A., Potyondi, D.O. and Lee, C.A. (1996), "Micromechanics-based models for fracture and breakout around the mine-by tunnel", *Proceedings of the Canadian Nuclear Society International Conference on Deep Geological Disposal of Neclear Waste*, Winnipeg.

Diederichs, M.S., Kaiser, P.K. and Eberhardt, E. (2004), "Damage initiation and propagation in hard rock during tunneling and the influence of near-face stress rotation", *Int. J. Rock Mech. Min. Sci.*, **41**, 785-812.

Emsley, S., Olsson, O., Stenberg, L., Alheid, H.J. and Falls, S. (1997), "ZEDEX – A study of damage and disturbance from tunnel excavation by blasting and tunnel boring", Swedish Nuclear Fuel and Waste Management CO.

Gehring, K.H. (1996), "Design criteria for TBM's with respect to real rock pressure. Tunnel boring machines—trends in design &

construction of mechanized tunneling", *International lecture series TBM tunnelling trends*, Rotterdam.

Harrison, J.P. and Hudson, J.A. (2000), Engineering rock mechanics: part 2: illustrative worked examples.

Hoek, E. and Bieniawski, Z.T. (1965), "Brittle fracture propagation in rock under compression", *Int. J. Fract. Mech.*, **1**(3), 137-155.

Hu, Y. and Randolph, M.F. (1998), "A practical numerical approach for large deformation problems in soil", *Int. J. Numer. Anal. Method. Geomech.*, **22**(5), 327-350.

International Tunnel Association (2000), "Recommendations and guidelines for tunnel boring machines (TBMs), Lausanne, Switzerland.

Kim, D. (2021), "Large deformation finite element analyses in TBM tunnel excavation: CEL and auto-remeshing approach", *Tunn. Undergr. Sp. Tech.*, **116**. https://doi.org/10.1016/j.tust.2021.104081.

Kim, D. and Jeong, S. (2021), "Estimation of the excavation damage zone in TBM tunnel using large deformation FE analysis", *Geomech. Eng.*, **24**(4), 323-335. https://doi.org/10.12989/gae.2021.24.4.323.

Kim, J., Ko, J. and Kim, D. (2023), "Analysis on inclined or rounded tip piles using 3D printing technology and FE analysis", *Geomech. Eng.*, **33**(1), 91-99. https://doi.org/10.12989/gae.2023.33.1.091.

Kwon SK, Lee CS, Cho SJ Jeon SW, Cho WJ. (2009), "An investigation of the excavation damaged zone at the KAERI underground research tunnel", *Tunnelling and Underground Space Technology*, **24**, 1-13.

Lee, G., Ryu, H., Cho, G. and Kwon, T. (2023), "Full-scale TBM excavation tests for rock-like materials with different uniaxial compressive strength", *Geomech. Eng.*, **35**(5), 487-497. https://doi.org/10.12989/gae.2023.35.5.487.

Lee, S.Y., Kim, D.H. and Jeong, S.S. (2016), "A study on the excavation damage zone (EDZ) under TBM advancement based on large deformation technique (Coupled Eulerian-Lagrangian)", *J. Korean Geotech. Soc.*, **32**(10), 5-13.

Martin, C.D. (1989), "Failure observations in situ stress domains at the underground research laboratory", *Proceedings of the Conference on Rock Mechanics and Rock Physics at Great Depth*, Pau France, **2**, Rotterdam, Balkema.

Martin, C.D. (1993), "The strength of massive Lac du Bonnet granite around underground openings", University of Manitoba.

Martin, C.D., Christiansson, R. and Soderhall, J. (2001), "Rock stability considerations for siting and constructing a KBS-3 repository: Based on experiences from Aspo HRL. AECL's URL, tunneling and mining", Swedish Nuclear Fuel and Waste Management CO..

Martin, C.D., Read, R.S. and Martino, J.B. (1997), "Observation of brittle failure around a circular test tunnel", *Int. J. Rock Mech. Min. Sci*., **34**(7), 1065-1073. https://doi.org/10.1016/S1365-1609(97)90200-8.

Martino, J.B. and Chandler, N.A. (2007), "Excavation-induced damage studies at the Underground Research Laboratory", *Int. J. Rock Mech. Min. Sci*., **41**(8), 1413-1426. https://doi.org/10.1016/j.ijrmms.2004.09.010.

Martino, J.B., Dixon, D.A., Kozak, E.T., Gascoyne, M., Vignal, B., Sugita, Y., Fujita, T. and Masumoto, K. (2007), "The tunnel sealing experiment: an international study of full-scale seals", *Phys. Chem. Earth*, **32**(1-7), 93-107. https://doi.org/10.1016/j.pce.2006.04.023.

Perras, M.A. and Diederichs, M.S. (2016), "Predicting excavation damage zone depths in brittle rocks", *J. Rock Mech. Geotech. Eng.*, **8**(1), 60-74. https://doi.org/10.1016/j.jrmge.2015.11.004.

Ramoni, M. and Anagnostou, G. (2011), "The interaction between shield, ground and tunnel support in TBM tunnelling through squeezing ground", *Rock Mech. Rock Eng.*, **44**(1), 37-61. https://doi.org/10.1007/s00603-010-0103-8.

Read, R.S. (2004), "20 years of excavation response studies at AECL's Underground Research Laboratory", *Int. J. Rock Mech. Min. Sci*., **41**(8), 1251-1275. https://doi.org/10.1016/j.ijrmms.2004.09.012.

Read, R.S., Chandler, N.A. and Dzik, E.J. (1998), "In situ strength criteria for tunnel design in highly-stressed rock masses", *Int. J. Rock Mech. Min. Sci.*, **35**(3), 261-278. https://doi.org/10.1016/S0148-9062(97)00302-1.

Saiang, D. (2004), "Damaged rock zone around excavation boundaries and its interaction with shotcrete", Licentiate Thesis, Department of Civil and Mining Engineering, Division of Rock Mechanics, Lulea University of Technology, Sweden.

Sakurai, S. (1983), "Displacement measurements associated with the design of underground openings", *Proceedings of the International Symposium of Field Measurements in Geomechanics*, Zurich.

Siren, T. (2015), "Excavation damage zones, fracture mechanics simulation and in situ strength of migmatitic gneiss and pegmatitic granite at the nuclear waste disposal site in Olkiluoto", Western Finland, Aalto University..

Stepansson, O., Shen, B., Rinne, M., Amemiya, K., Yamashi, R. and Toguri, S. (2008), "FRACOD modeling of rock fracture and permeability change in excavation damaged zones", *Proceedings of the 12th International Conference of International Association for Computer Methods and Advances in Geomechanics (IACMAG)*, 1048-1059.

Sun, B., Yang, H., Zeng, S., Yin, Y. and Fan, J. (2023), "Crack initiation mechanism and meso-crack evolution of pre-fabricated cracked sandstone specimen under uniaxial loading", *Geomech. Eng.*, **33**(6), 597-609. https://doi.org/10.12989/gae.2023.33.6.597.

Tian, Y., Cassidy, M.J., Randolph, M.F., Wang, D. and Gaudin, C. (2014), "A simple implementation of RITSS and its application in large deformation analysis", *Comput. Geotech.*, **56**, 160-167. https://doi.org/10.1016/j.compgeo.2013.12.001.

Wang, D., Bienen, B., Nazem, M., Tian, Y., Zheng, J., Pucker, T. and Randolph, M. (2015), "Large deformation finite element analyses in geotechnical engineering", *Comput. Geotech.*, **65**, 104-114. https://doi.org/10.1016/j.compgeo.2014.12.005.

Xu, H. and Arson, C. (2014), "Anisotropic damage models for geomaterials: Theoretical and numerical challenges", *Int. J. Comput.ational Method.*, **11**(2), https://doi.org/10.1142/S0219876213420,073.

Zhao, K., Janutolo, M. and Barla, G. (2012), "A completely 3D model for the simulation of mechanized tunnel excavation", *Rock Mech. Rock Eng.*, **45**(4), 475-497.